Neurotoxicology 70 (2019) 99–111

Contents lists available at ScienceDirect

Neurotoxicology

journal homepage: www.elsevier.com/locate/neuro

Full Length Article

Otilonium and pinaverium trigger mitochondrial-mediated apoptosis in rat embryo cortical neurons in vitro

Fernanda García-Alvarado[a,b,c], Giulia Govoni[a,b], Ricardo de Pascual[a,b], Cristina Ruiz-Ruiz[a,b], Alicia Muñoz-Montero[a,b], Luis Gandía[a,b], Antonio M.G de Diego[a,d], Antonio G. García[a,b,c,d,*]

[a] Instituto Teófilo Hernando, Arzobispo Morcillo, 4, 28029, Madrid, Spain
[b] Departamento de Farmacología y Terapéutica, Facultad de Medicina, Universidad Autónoma de Madrid, Arzobispo Morcillo, 4, 28029, Madrid, Spain
[c] Instituto de Investigación Sanitaria, Hospital Universitario de La Princesa, Diego de León, 62, 28006, Madrid, Spain
[d] DNS Neuroscience, Parque Científico de Madrid, Faraday, 7, Campus de Cantoblanco. 28049, Madrid, Spain

ARTICLE INFO

Keywords:
Otilonium
Pinaverium
Apoptosis
Mitochondria
Cortical neurons

ABSTRACT

In the frame of a repositioning programme with cholinergic medicines in clinical use searching for neuroprotective properties, we surprisingly found that spasmolytic antimuscarinics otilonium and pinaverium exhibited neurotoxic effects in neuronal cultures. We decided to characterize such unexpected action in primary cultures of rat embryo cortical neurons. Neurotoxicity was time- and concentration-dependent, exhibiting approximate EC_{50} values of 5 μM for both drugs. Seven antimuscarinic drugs endowed with a quaternary ammonium, and another 10 drugs with different cholinergic activities, carrying in their molecule a ternary ammonium did not exhibit neurotoxicity. Both drugs caused a concentration-dependent blockade of whole-cell inward currents through voltage-activated calcium channels (VACCs). Consistent with this, they also blocked the K^+-elicited $[Ca^{2+}]_c$ transients. Neither antioxidant catalase, glutathione, n-acetylcysteine, nor melatonin protected against neurotoxicity of otilonium or pinaverium. However cyclosporine A, a blocker of the mitochondrial permeability transition pore, prevented the neurotoxic effects of otilonium and pinaverium monitored as the fraction of cells undergoing apoptosis. Furthermore, the caspase-9 and caspase-3 inhibitor Ac-LEHD-CHO mitigated the apoptotic neuronal death of both drugs by around 50%. Data are compatible with the hypothesis that otilonium and pinaverium elicit neuronal death by activating the intrinsic mitochondrial-mediated signaling pathway of apoptosis. This may have its origin in the mitigation of Ca^{2+} entry and the uncoupling of the Ca^{2+}-dependent generation of mitochondrial bioenergetics, thus causing the opening of the mitochondrial mPTP to elicit apoptotic neuronal death.

1. Introduction

Since long, spasmolytics antimuscarinic otilonium and pinaverium are widely being used in patients suffering of irritable bowel syndrome (Ford et al., 2018; Lovell and Ford, 2012). Otilonium bromide (*N,N*-diethyl-*N*-methyl-2-[(4-benzoyl)oxy]ethanaminium) is a quaternary ammonium derivative with a long aliphatic chain. For years, otilonium bromide has been widely used as a spasmolytic agent for intestinal disorders (Barbara et al., 1991; Evangelista et al., 2018). Its intestinal smooth muscle relaxant effect has been attributed to its ability to block muscarinic receptors (Maggi and Meli, 1983b; Traini et al., 2017) as well as to its capacity of interfering with Ca^{2+} entry through voltage-activated calcium channels (VACCs) and the release of Ca^{2+} from intracellular stores (Giachetti, 1991; Maggi and Meli, 1983a; Martinez-Cutillas et al., 2013). Additionally, the blockade of neuronal nicotinic receptors in bovine chromaffin cells (Gandia et al., 1996a) suggests that the blockade of those receptors at parasympathetic ganglia of the Auerbach plexus might also contribute to the spasmolytic effects of otilonium. Blockade of VACCs of the L-, N-, and PQ-subtypes (Gandia et al., 1996a) might also contribute to those clinically useful effects. Additionally, otilonium blocks muscarinic and tachykinin receptors in smooth muscle and primary afferent neurons (Cipriani et al., 2015; Santicioli et al., 1999). The fact that otilonium has a quaternary ammonium explains its poor gastrointestinal absorption due to high

* Corresponding author at: Instituto Teófilo Hernando, Departamento de Farmacología y Terapéutica, Facultad de Medicina, Universidad Autónoma de Madrid, Arzobispo Morcillo, 4. 28029, Madrid, Spain.
E-mail addresses: fernanda.garcia@estudiante.uam.es (F. García-Alvarado), giuli.govoni@student.unife.it (G. Govoni), ricardo.pascual@uam.es (R. de Pascual), cristina.ruizr@estudiante.uam.es (C. Ruiz-Ruiz), alicia.munnozm@uam.es (A. Muñoz-Montero), luis.gandia@uam.es (L. Gandía), antoniomiguel.garcia@dnsneuroscience.es, agg@uam.es (A.G. García).

https://doi.org/10.1016/j.neuro.2018.11.003
Received 20 July 2018; Received in revised form 6 November 2018; Accepted 6 November 2018
Available online 15 November 2018
0161-813X/

polarity, thus precluding any systemic ganglionic blocking action and/or side effects associated to muscarinic receptor blockade.

On the other hand, pinaverium bromide (4-[(2-bromo-4, 5 dimethoxyphenyl) methyl]-4-[2-[2-(6, 6-dimethyl-4-bicyclo [3.1.1] heptanyl) ethoxy] ethyl] morpholin-4-ium), is an antimuscarinic quarternary ammonium drug that blocks L-type VACCs with selectivity for the gastrointestinal tract (Bobo et al., 1994; Bouchoucha et al., 2000; Feron et al., 1992). As otilonium, pinaverium blocks muscarinic receptors (Malysz et al., 1997) and is used as spasmolytic in intestinal disorders (Lovell and Ford, 2012).

In the frame of a drug repositioning programme looking for neuroprotective properties of about 30 cholinergic medicines in clinical use, we found that otilonium and pinaverium decreased cell viability in primary cultures of rat embryo cortical neurons. The purpose of this investigation was the characterization of such effects. We have found that both drugs caused a time- and concentration-dependent apoptotic neuronal death. The mechanism underlying such an action seems to be linked to the activation of the intrinsic mitochondrially-mediated pathway of apoptosis through the opening of the mitochondrial permeability transition pore (mPTP) and the subsequent activation of caspases.

2. Material and methods

2.1. Cell culture

2.1.1. Isolation and culture of cortical neurons

All experiments were carried out in accordance with the code of ethics and guidelines established by the European Community Directive (2010/63/EU) and Spanish legislation 1201/2005. All animals used in this study were provided by the local university's facilities where they were housed (EX 021-U). All efforts were made to minimize the number of animals and their suffering.

Experiments were performed in cortical neurons prepared from brains of embryos of 18 days pregnant Sprague-Dawley rats (250–300 g weight). Rats were killed by decapitation under anesthesia with sodium pentobarbital (60 mg/kg i.p.), and the embryo heads were placed in 1x PBS (phosphate buffered saline). Tissues were gently removed using tongs and scissors, and the cerebral cortex was carefully dissected out after removing the skull of the head of the embryo, and transferred to ice-cold in a little Petri dish with Neurobasal (medium supplemented with 5 mL L-glutamine, 50 IU/mL penicillin, 50 µg/mL streptomycin, gentamicin 10 mg/mL and 10% fetal bovine serum (FBS)); cerebral cortex pieces were dissociated in 2 mL MEM (supplemented with 10% FBS) using a Pasteur pipette. After centrifugation, cells were resuspended in another 2 mL MEM (supplemented with 10% FBS), and after cell counting with a Neubauer chamber at the microscope, cells were seeded with a density of 60.000 cells/well in treated plastic plaques of 48 wells. Cultures were maintained at 37 °C in humified 5% CO_2/95% air atmosphere. After 3 h, culture medium was changed to Neurobasal containing B-27 supplement (2%) in the absence of serum and incubated for 6–8 days, the time range in which the experiments were performed.

2.1.2. Culture of bovine chromaffin cells (BCCs)

BCCs were isolated from adrenal glands of calves (*taurus*), according to standard methods with some modifications (Moro et al., 1990). After digestion of the adrenal medulla with collagenase, purification of BCCs was achieved by several consecutive centrifugations. Cells were suspended in Dulbecco's modified Eagle's medium (DMEM) supplemented with 5% fetal bovine serum, 50 IU/mL penicillin, and 50 µg/mL streptomycin. To prevent the excessive growth of fibroblasts, proliferation inhibitors (10 µM cytosine arabinoside, 10 µM fluorodeoxyuridine, and 10 µM leucine methyl ester) were added to the medium. Cells were seeded in 48-well plates and kept at 37 °C in an incubator under an atmosphere of 5% CO_2 and 95% air atmosphere.

2.1.3. Culture of SH-SY5Y cells

SH-SY5Y cells were maintained in a 1:1 mixture of F-12 nutrient mixture (Ham 12) and Eagle MEM supplemented with 15 nonessential amino acids, 1 mM sodium pyruvate, and 10% heat-inactivated FBS, 50 IU/mL penicillin, and 50 µg/mL streptomycin. Cultures were seeded into flasks containing supplemented medium and kept at 37 °C in a humidified atmosphere of 5% CO_2 and 95% air. For assays, SH-SY5Y cells were subcultured in 48-well plates at a seeding density of 1×10^5 cells/well. Cells were treated with the drugs before confluence in MEM/F-12 with 1% FBS. Cells were used at passages below 13.

2.2. Quantification of cell viability by MTT

Cell viability was measured by a quantitative colorimetric assay by using the MTT based method (3-[4, 5-dimethylthiazo1-2-y1]-2, 5-diphenyltetrazolium bromide) (Mosmann, 1983). MTT (Sigma-Aldrich, Madrid, Spain) was added into the wells (0.5 mg/mL) and incubated at 37 °C for 15 min. The tetrazolium ring of MTT can be cleaved by active dehydrogenases to produce a precipitated formazan that was solubilized with DMSO; cellular viability was quantified in a colorimetric reader at 540 nm (FLUOstar Optima, BMG, Ortenberg, Germany). Data were expressed as percentage of MTT reduction, taking the maximum control cell capability in each individual experiment as 100%.

2.3. Measurement of apoptosis and necrosis with annexin V–phycoerythrin (PE)/7-amino-actinomycin-D (7-AAD) double staining

Apoptosis was determined by flow cytometry using fluorescein isothiocynate (FITC)-labelled annexin V; this was used in combination with a vital dye such as 7-amino-actinomycin D (7-AAD). An annexin V–PE and 7-AAD double staining kit (BD Bioscience, Madrid, Spain) was used according to the manufacturer's instructions. Briefly, at the end of the experiment, cells were collected by centrifugation and resuspended in 100 µL of 1 × binding buffer with 5 µL annexin V–PE and 5 µL 7-AAD. After incubation at room temperature for 15 min in the dark, 400 µL of 1 × binding buffer was added. Cells were then subjected to FACS analysis (Beckman Coulter, Madrid, Spain). At least 20,000 events per assay well were included and represented as dot plots. Annexin +/7-AAD − cells were considered early apoptotic cells, annexin+/7-AAD + late apoptotic cells, and annexin−/7-AAD − were viable cells (Schmid et al., 1992).

2.4. Whole-cell current recordings

Coverslips containing the cells were placed on an experimental chamber mounted on the stage of a Nikon Diaphot inverted microscope. Cells were continuously superfused with a control Krebs-HEPES solution composed of (in mM) 145 NaCl, 1.2 $MgCl_2$, 5.6 KCl, 2 $CaCl_2$, 10 HEPES and 11 glucose (pH 7.4, NaOH). Inward currents through voltage-activated calcium channels (VACCs) were recorded using the voltage-clamp mode of the whole-cell configuration of the patch-clamp technique (Hamill et al., 1981), using 10 mM Ba^{2+} as ion carrier in order to increase the current amplitude (I_{Ba}). Whole-cell recordings were made with fire-polished borosilicate pipettes (resistance 5–9 MΩ) that were mounted on the headstage of an EPC-9 patch-clamp amplifier (HEKA Electronik, Lambrecht, Germany), allowing cancellation of capacitative transients and compensation of series resistance. Data were acquired with a sample frequency of 20 kHz by using PULSE v8.74 software (HEKA Elektronik). Data analyses were performed with PULSE v8.74 programs (HEKA Elektronik).

To monitor I_{Ba} cells were internally dialysed with an intracellular solution containing (in mM): 100 Cs-glutamate, 14 EGTA, 20 TEA-Cl, 10 NaCl, 5 Mg-ATP, 0.3 Na-GTP, and 20 HEPES (pH 7.3, CsOH). The external solutions were rapidly exchanged using electronically driven miniature solenoid valves coupled to a multi-barrel concentration clamp device, the common outlet of which was placed within 100 µm of

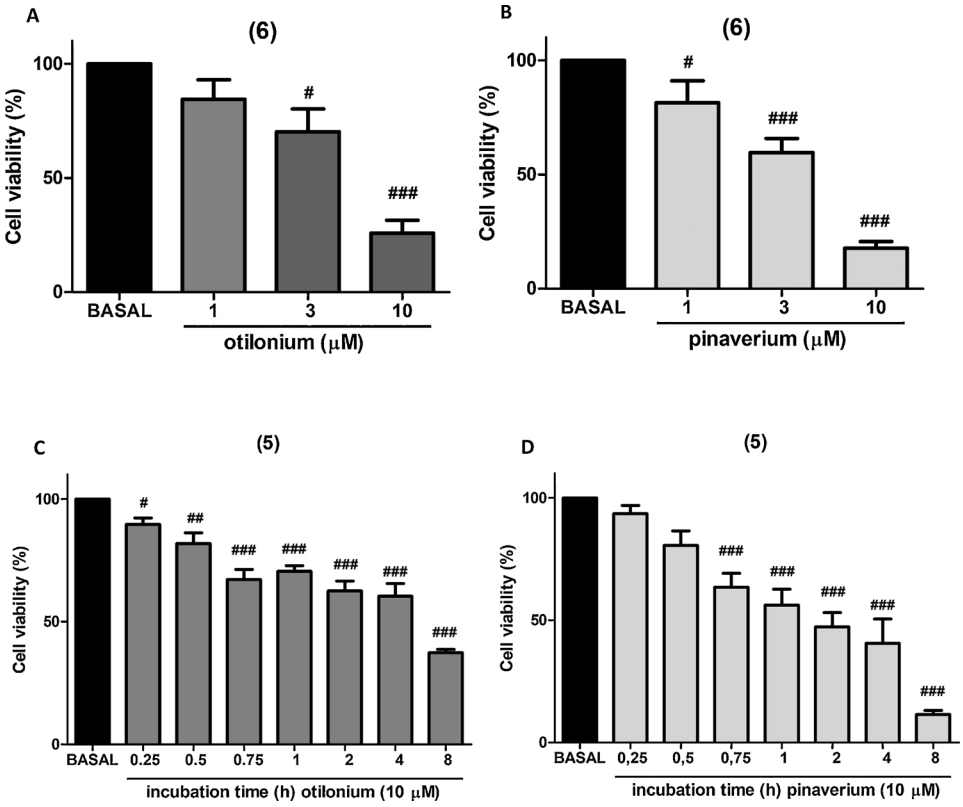

Fig. 1. Neurotoxic effects of otilonium and pinaverium: concentration and time dependence. In panels A and B, neurons (7–10 DIV) were incubated during 24 h in Neurobasal medium containing no drugs (BASAL) or increasing concentrations of otilonium or pinaverium (abscissae). In panels C and D, neurons were incubated respectively with otilonium or pinaverium (10 μM) during the time periods shown in abscissae. Cell viability was estimated with MTT at the end of their respective incubation periods in the four panels (ordinates, expressed in % BASAL). Data are mean ± SEM of the number of triplicate experiments made on different cultures shown in parentheses. #p < 0.05, ## p < 0.01, ###p < 0.001 with respect BASAL.

the cell to be patched. The flow rate was 1 mL/min and was regulated by gravity.

In order to measure the inward I_{Ba}, cells were held at −80 mV. I_{Ba} was generated by 50 ms depolarising pulses at 10 mV every 10 s. All experiments were performed at room temperature (24 ± 2 °C) on cells from 6 to 10 days after culture.

2.5. Measurement of cytosolic calcium levels in cell populations

Basal and K^+-stimulated changes of cytosolic calcium concentrations ($[Ca^{2+}]_c$) were monitored in cell populations. Cell populations were loaded with 3 μM Fluo-4 AM in Krebs-HEPES solution, with the following composition (in mM): NaCl 144, KCl 5.9, $MgCl_2$ 1.2, $CaCl_2$ 2, glucose 11 and HEPES 10 at pH 7.4, for 45 min at 37 °C. The changes in basal $[Ca^{2+}]_c$ and stimulated $[Ca^{2+}]_c$ elevations were monitored by placing the 96-well plate containing the cells (50,000 cell/well) in a spectrofluorimeter plate reader (FLUOstar optima) at 37 °C, at 485 nm excitation wavelength and at 505 nm emission wavelength. The response of each well was calibrated by measuring the maximum and minimum values of fluorescence by the addition of Triton X-100 to 5% (F_{max}), followed by 1 mM $MnCl_2$ (F_{min}). Data on F_{max}-F_{min} were normalized to 100% in each cell batch plate; the relative fluorescence of cells subjected to a K^+ challenge, in the absence or the presence of increasing concentrations of otilonium or pinaverium, were expressed as % of the F_{max}-F_{min} within each 96-well plate. In this manner, the variations between different plates and cultures were minimized.

2.6. Measurement of cytosolic calcium transients at the single-cell level

To measure $[Ca^{2+}]_c$ transients in rat embryonic cortical neurons stimulated with 35 mM K^+, cells plated on coverslips were incubated for 1 h at 37 °C in DMEM medium containing the calcium probe fura-2 acetoxymethyl ester (fura-2 AM, 5 μM). Thereafter, coverslips were mounted in a chamber and cells were washed and covered with Tyrode's solution. The setup for microfluorescence monitoring consisted in a Leica DMI 4000B inverted light microscope (Leica Microsystems, Barcelona, Spain) equipped with an oil immersion objective (Leica 40X Plan Apo, numerical aperture 1.25). Then, cells were continuously superfused by means of a five-way system with a common outlet 0.28-mm tube driven by electrically controlled valves, with Tyrode's solution at room temperature and 1 mL/min. Fura-2 was alternatively excited at 340 ± 10 and 380 ± 10 nm, using a Küber CODIX xenom arc lamp (Leica). Emitted fluorescence was measured at 540 ± 20 nm and quantified with an intensified charge coupled device camera (Hamamatsu camera controller C10600 ORCA R2). Fluorescence images were generated at 1 s intervals and all experiments were performed at room temperature.

2.7. Drugs and solutions

L-glutamic acid monosodium salt, otilonium bromide, oxybutynin chloride, trimebutine, biperiden, orphenadrine, trihexyphenidyl hydrochloride, atropine, edrophonium, neostigmine, pyridostigmine, butylscopolamine, propantheline, procyclidine, aclidinium bromide, glycopirronium bromide, ipratropium bromide, tiotropium bromide, caspase 9 inhibitor Ac-LEHD-CHO, cyclosporin A and staurosporine were obtained from Sigma-Aldrich (Madrid, Spain). Media for cell cultures were purchased from Thermo Fisher Waltham (Massachusetts, USA). MK801 was obtained from Ascent Scientific (Cambridge, UK). B27 was purchased from GIBCO (Grand Island, NY, USA).

2.8. Statistics

Data are expressed as means ± SEM of the number of experiments from different cultures shown in each graph. Each treatment and controls were done in triplicate (3 wells within each plaque) that were averaged to give a n = 1 within each individual plate. Student's *t*-test for paired data were applied (controls and treatments were always included in each 48-well plate). The D´Agostino-Pearson *t*-test was used for paired data comparisons (namely, control versus a given treatment)

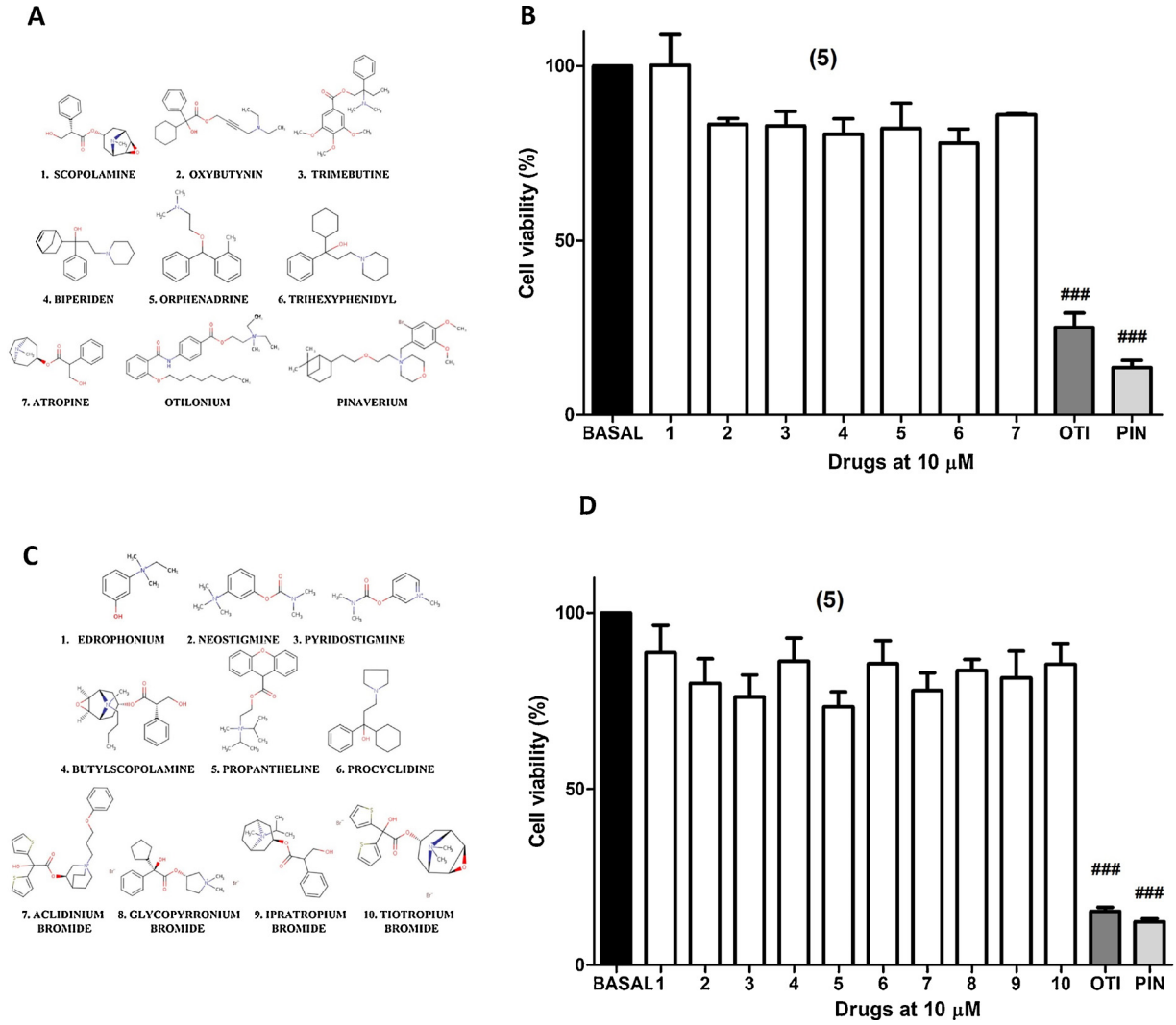

Fig. 2. Cholinergic drugs on neuronal viability. Neurons were incubated for 24 h with 10 μM of each drug; otilonium (OTI) and pinaverium were also included for comparative purposes. Cell viability was monitored with MTT at the end of the incubation period (ordinate, expressed as % of BASAL). A, molecular structure of antimuscarinic drugs with a tertiary ammonium; B, effects of these drugs on neuronal viability; C, molecular structure of cholinergic drugs with a quaternary ammonium; D, effects of these drugs on neuronal viability. Data are means ± SEM of the number of triplicate experiments from different neuronal cultures shown in parentheses. ###$p < 0.001$ with respect to BASAL.

within the same experiment. The comparisons between experimental and control groups were performed by one-way ANOVA followed by Tukey post-hoc test, as required. For not normal data, Kruskal-Wallis test was used followed by Dunn's multiple comparison test. Differences were considered to be statistically significant when $p < 0.05$. All statistical procedures were carried out using GraphPad Prism 5.0 (GraphPad Software, Inc., La Jolla, CA).

3. Results

3.1. Concentration- and time-dependent neurotoxic effects of otilonium and pinaverium

Most experiments were performed in cortical neurons of 7–10 DIV. There conditions are widely used in experiments on neuronal death and neuroprotection (Choi, 1985). We first tested the effects of otilonium and pinaverium on the viability of neurons. To this aim, neurons were exposed to increasing concentrations of otilonium or pinaverium for 24 h in Neurobasal medium. After this period, cell viability was estimated with MTT. "Threshold" neurotoxicity was found to be 1 μM for both compounds, with a 15–18% decrease in cell viability, which was stadistically significant in the case of pinaverium with respect to basal conditions (Fig. 1A,B). At 3 μM, however, otilonium and pinaverium caused 30% and 40.3% cell loss (otilonium $p < 0.05$ and 0.001 pinaverium) with respect basal ($n = 6$); and finally, at 10 μM otilonium elicited 74% cell loss and pinaverium caused 82% cell loss (Fig. 1A,B).

We next explored the time course of the neurotoxic effects of both agents. This was aimed at finding out whether such effects were due to rapid non-specific necrotic effects or whether those actions were mediated by the activation of a more selective apoptotic signaling pathway. Neurons were incubated with 10 μM otilonium or pinaverium for time periods ranging from 15 min to 8 h. At the end of these periods, cell viability was estimated with the MTT assay. Fig. 1C,D summarizes the results from 5 experiments. In the case of otilonium, there was a small (10%) but significant decay of cell viability after only 15 min of cell incubation. This loss was gradual and time-dependent at 30 and 45 min, reaching a plateau in the range of 1 to 4 h (around 30–40% cell loss). Cell damage rose to 63% after 8 h incubation (Fig. 1C).

The time-dependent damaging effect of pinaverium was close to linear in the range of 15 min to 4 h, although cell loss at 15 and 30 min (about 6–20%) did not reach the level of statistical significance. After 8 h incubation, pinaverium elicited over 90% cell loss. Thus once more,

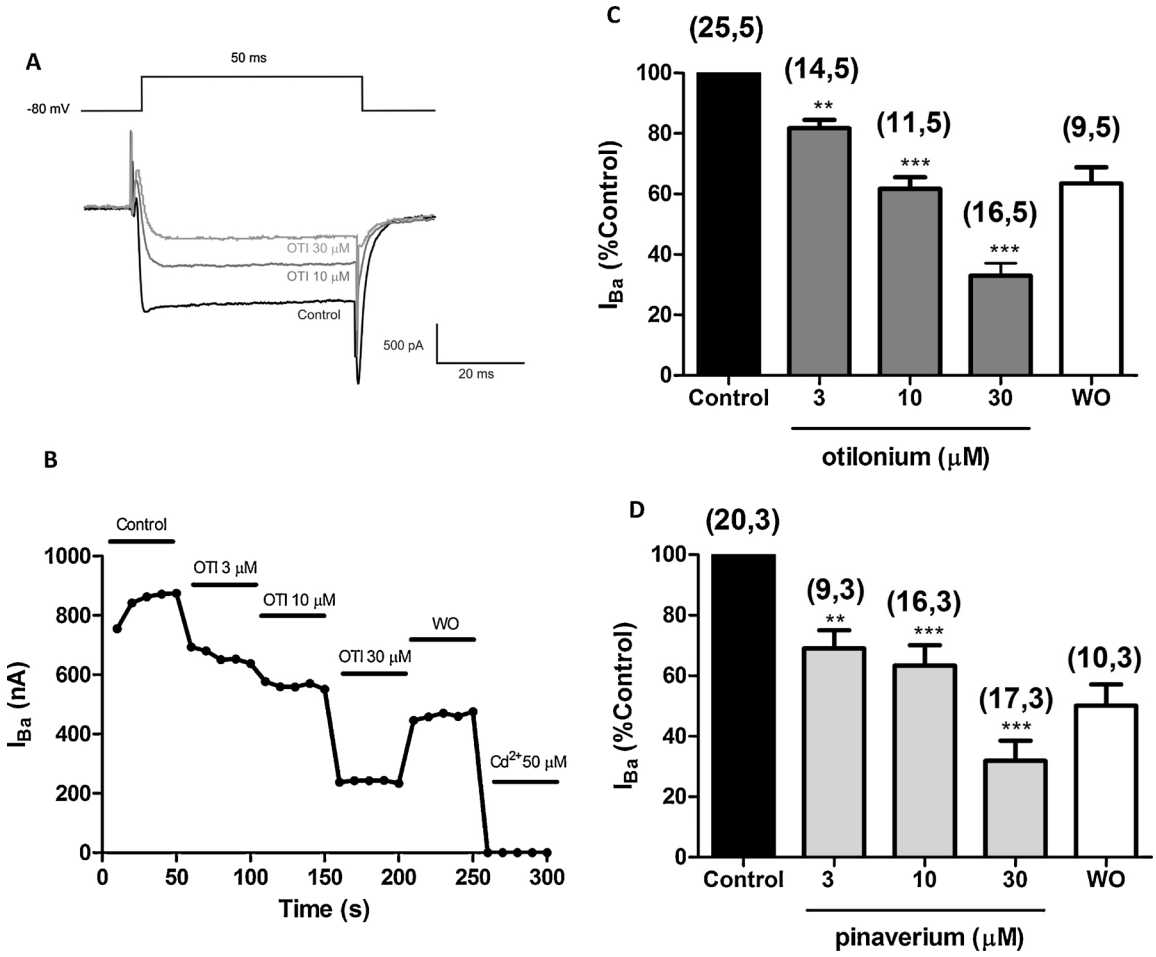

Fig. 3. Effects of otilonium and pinaverium on Ba^{2+} inward currents through voltage-dependent calcium channels. Whole-cell inward Ba^{2+} currents were recorded in neurons voltage-clamped at -80 mV. Currents were elicited by 50 ms depolarizing pulses to 10 mV applied at 10 s intervals. A, Typical inward current traces from a cell before (control) and in the presence of increasing concentrations of otilonium cumulatively added.B, Representative time course of I_{Ba} in a typical cell, before and during cell exposure to increasing concentrations of otilonium (horizontal bars). C, Pooled data on the blockade of I_{Ba} (normalized as % control, ordinate) at the different concentrations of otilonium tested (bottom of each column). D, Pooled data on the blockade of I_{Ca} (normalized as % control, ordinate) at different concentrations of pinaverium tested (bottom of each column). Data in panels C and D are means ± SEM of the number of cells from 5 (C) and 3 (D) different cultures shown in parentheses. **p < 0.01; ***p < 0.001 with respect to control. (One-way ANOVA, Tukey´s multiple comparison test).

pinaverium seemed to exhibit greater potency and reliability in eliciting neuronal damage, compared to otilonium (Fig. 1C,D).

3.2. Effects of cholinergic drugs other than otilonium and pinaverium, on cell viability

Two possibilities emerged when trying to explain the neurotoxic effects of otilonium and pinaverium on neurons: (1) they were linked to their muscarinic receptor blocking effects and (2) the fact that they could be associated to a common structural molecular family, because they are endowed with a quaternary ammonium. To test both hypothesis, we selected 7 drugs from our repositioning program that are recognized to have antimuscarinic effects and another 10 drugs having in common a quaternary ammonium but with different cholinergic activities.

In 5 experiments we tested if the antimuscarinic drugs scopolamine, oxybutynin, trimebutine, biperiden, orphenadrine, trihexyphenidyl and atropine (all at 10 μM during 24 h) exhibited neurotoxic effects in cultures of cortical neurons. We found that scopolamine did not cause cell loss. However, the other 6 drugs elicited about 20% cell loss; nevertheless, when compared with basal this loss of cell viability did not reach the level of statistical significance. We also incubated in parallel cell wells incubated with 10 μM otilonium and pinaverium that caused their expected cell damage, 75% and over 90% cell loss, respectively (Fig. 2B).

In another series of experiments we tested 10 cholinergic drugs having a quaternary ammonium. Three of them were inhibitors of acetylcholinesterase (AChase, Fig. 2C drugs 1, 2, 3) and the other 7 were antimuscarinic drugs (drugs 4–10 in Fig. 2C). Cells were incubated for 24 h with 10 μM of the 3 AChase inhibitors (edrophonium, neostigmine, pyridostigmine) and of the 7 antimuscarinic compounds (butylscopolamine, propantheline, procyclidine, aclidinium bromide, glycopyrronium bromide, ipratropium bromide and tiotropium bromide). As in the case of non-polar drugs (Fig. 2A), these polar cholinergic compounds caused about 10–25% cell loss, as indicated in the bar graph drawn with averaged data of 5 triplicated experiments; however, in no case this decay in cell viability reached the level of statistical significance, with respect the 100% value of basal viability. Again, otilonium and pinaverium caused their expected cell damaging effects, over 80–90% cell loss (Fig. 2D).

3.3. The neurotoxic effects of otilonium and pinaverium are unaffected by MK801, melatonin, N-acetylcysteine, donepezil and catalase

In searching for the signaling pathways likely involved in the neurotoxic effects of otilonium and pinaverium, we explored the calcium

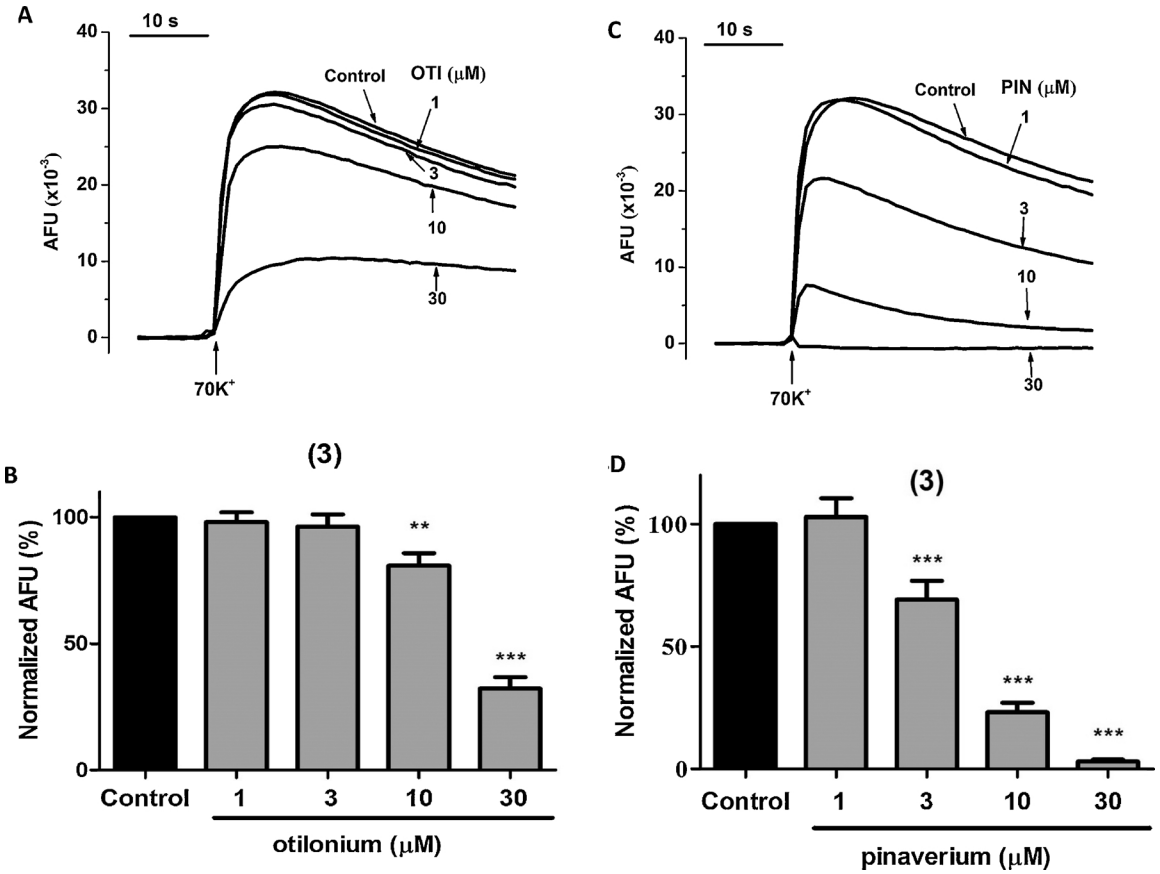

Fig. 4. Blockade by otilonium and pinaverium of the elevation of cytosolic Ca^{2+} ($[Ca^{2+}]_c$) elicited by K^+ depolarization of neurons, monitored as arbitrary fluorescence units (AFU, ordinates). Neurons seeded in 96-well plates were loaded with fluo-4 AM. Then, experiments were performed in a plate fluorescence reader. After 1 min stabilization of basal fluorescence, neurons were challenged with high K^+(70 mM) in the absence (control $[Ca^{2+}]_c$ transient) and the presence of increasing concentrations of otilonium or pinaverium, as indicated in the original records (panels A, C) and at the bottom of bar graphs. Each variable was tested in sextuplicate within each plate. Data in panels B and D are means ± SEM of 3 sextuplicate experiments done in different cultures. **p < 0.01, ***p < 0.001, with respect control neurons.

overloading hypothesis using the NMDA receptor blocker MK801, antioxidants melatonin, *N*-acetylcysteine (NAC) and catalase, as well as the neuroprotective AChase inhibitor donepezil. Neurons were subjected to a two-step protocol: first they were incubated for a 24 h period with putative neuroprotective agents and subsequently they were incubated for an additional 24 h period with increasing concentrations of otilonium or pinaverium, still in the presence of those agents. None of those compounds affected the neurotoxic effects of these two drugs (data not shown).

3.4. Blockade by otilonium and pinaverium of inward currents through voltage-activated calcium channels

Although scarce, some data in the literature suggest that otilonium and pinaverium block the VACC currents. This is the case for otilonium in intestinal smooth muscle (Giachetti, 1991) and chromaffin cells (Gandia et al., 1996a). Pinaverium also blocks the ileal smooth muscle L-type VACCs (Feron et al., 1992). As VACCs currents in cortical neurons have not been reported to be affected by otilonium and pinaverium and, if blocked, this effect could contribute to its neurotoxic effects, we here studied whether both drugs affected the inward current through VACCs of cortical neurons voltage-clamped at -80 mV. Barium ions were used as ion carriers to enhance current amplitude (Gandia et al., 1996b). Currents were evoked by intermittent depolarizing pulses to 10 mV applied at 10 s intervals. Fig. 3A shows example I_{Ba} traces obtained from a neuron before (control) and after 1 min of cumulative exposure to 10 μM or 30 μM otilonium.

Current underwent no inactivation (note we are recording in the presence of Ba^{2+}); at 10 μM the current was blocked by 38.2% and at 30 μM the blockade increased to 67.0%. Fig. 3B displays the time course of I_{Ba} recorded from an example neuron showing a concentration-dependent blockade of I_{Ba} elicited by cumulative neuronal exposure to increasing otilonium concentrations. Washout of the 30 μM otilonium gave rise to only a partial current recovery and 50 μM Cd^{2+} suppressed I_{Ba},. Similar experiments were done with pinaverium but for the sake of brevity they were not graphed.

Pooled data on normalized current blockade show that otilonium inhibited I_{Ba} in a concentration-dependent manner, with a partial current reversal and an IC_{50} of 14.8 μM (Fig. 3C). The same occurred with pinaverium that blocked I_{Ba} with IC_{50} of 14.0 μM and a partial current recovery upon washout (Fig. 3D).

3.5. Blockade by otilonium and pinaverium of the K^+-elicited cytosolic Ca^{2+} elevations in neuronal populations

Consistent with the blockade of VACC currents, otilonium and pinaverium should also block the cytosolic Ca^{2+} elevations ($[Ca^{2+}]_c$) elicited by neuronal challenging with 70 mM K^+ that, according with the Nernst equation, will fully depolarize the cell to open such VACCs. We first performed experiments of global $[Ca^{2+}]_c$ elevations in neuronal populations (50.000 neurons per well, plated in 96-well black plates).

Neurons loaded with the Ca^{2+} probe fluo-4 and stimulated with 70 mM K^+ (low Na^+) responded with a healthy $[Ca^{2+}]_c$ elevation that

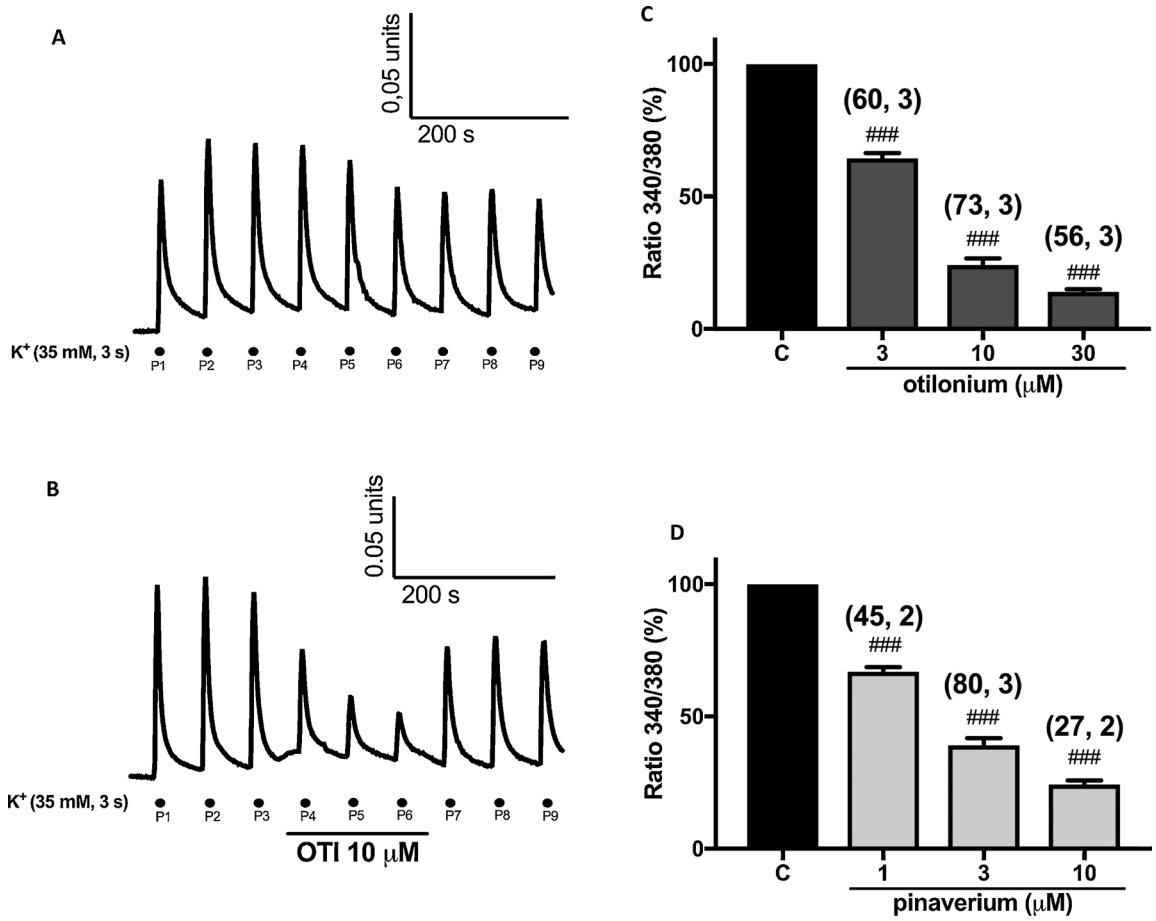

Fig. 5. Measurements of cytosolic calcium transients $[Ca^{2+}]_c$ in single cortical neurons loaded with fura-2, upon stimulation with 35 mM K^+ and perfusion with varying concentrations of otilonium and pinaverium. A, Original recording of $[Ca^{2+}]_c$ upon stimulation with pulses of 35 mM K^+ for 3 s. Cells were stimulated with 9 K^+ pulses applied every 60 s. B, Original recording of $[Ca^{2+}]_c$ upon stimulation with pulses of 35 mM K^+ for 3 s. Cells were stimulated with 9 K^+ pulses applied every 60 s and 10 μM otilonium perfusion was started as shown in the graph. Pulses 2 and 5 of each recording were compared to analyze the effect of otilonium perfusion. C, Effect of the perfusion of varying otilonium concentrations (3, 10 and 30 μM) on $[Ca^{2+}]_c$, measured by the fluorescence ratio 340/380. Results are expressed as a percentage of the control, considering this value as 100%. D, Effect of varying pinaverium concentrations (1, 3 and 10 μM) on $[Ca^{2+}]_c$. Results are expressed as a percentage of control, considering this value as 100%. ***P < 0.001 (D'Agostino &Pearson normality test, Kruskal-Wallis test and Dunn's multiple comparison test).

slowly faded off, likely due to Ca^{2+}-dependent inactivation of VACCs. At 1–3 μM, otilonium did not affect the peak $[Ca^{2+}]_c$ elevations; however, at 10 and 30 μM otilonium blocked such signal by 19.7% and 67.8%, respectively (Fig. 4A,B). Pinaverium was somehow more potent because at 3, 10 and 30 μM caused the inhibition of the K^+-elicited $[Ca^{2+}]_c$ transient by 30.8%, 76.8%, and 97%, respectively (Fig. 4C,D).

3.6. Blockade by otilonium and pinaverium of K^+- elicited cytosolic calcium transients in single neurons

To further inquire about the capacity of otilonium and pinaverium to block the $[Ca^{2+}]_c$ transients, we did experiments in single neurons loaded with fura-2. Neurons were intermittently stimulated with 3 s pulses of a 35 mM K^+ solution applied at 1 min intervals. Under these conditions, a $[Ca^{2+}]_c$ transient was obtained that was quite stable during the first 5 pulses and then gradually decreased at pulses P6 to P9. This could be due to the fact that at 1-min interval pulsing the basal $[Ca^{2+}]_c$ remained mildly elevated, thus contributing to inactivation of VACCs in subsequent K^+ pulses (Fig. 5A). When otilonium at 10 μM was perfused through the cell surface for a minute, a pronounced gradual depression of the transient at P4-P6 was produced. A notable recovery was promptly produced upon drug washout (Fig. 5B). Similar experiments were done with pinaverium but for the sake of brevity, an example record is not presented.

Pooled data on the effects of otilonium and pinaverium on the K^+-elicited $[Ca^{2+}]_c$ transients are graphed in Fig. 5 C,D. Both drugs produced a concentration-dependent blockade of those transients with estimated IC_{50} values for otilonium and pinaverium of 4.6 μM and 2.0 μM, respectively. These results at the single-cell level are more nitid than those obtained in cell populations. In cell population experiments, the K^+ stimulus was a strong 70 mM which would depolarize the cell to near 0 mV, around the peak Ca^{2+} current for voltage-dependent calcium channels. Whereas in single cell the stimulus was a much milder $35K^+$. It is probable that with the $70K^+$ stimulus, which remains in the well bathing the cells after injection, the amount of Ca^{2+} entering the cell was such that reached saturating concentrations of the probe fluo-4. A mild blockade of Ca^{2+} entry under these conditions would not suffice to reduce $[Ca^{2+}]_c$ to the effective working range of the probe. On the other hand, with the milder $35K^+$ stimulation, and stimulus times of 3-s and wash, fura-2 would still be in non-saturating working range being able to detect smaller decreases in $[Ca^{2+}]_c$.

3.7. Cyclosporine A mitigates the neurotoxic effects of otilonium and pinaverium

Next we explored whether cyclosporine A (CSA), a blocker of the mitochondrial permeability transition pore (mPTP) (Osman et al., 2011), could affect the neurotoxic effect of otilonium and pinaverium.

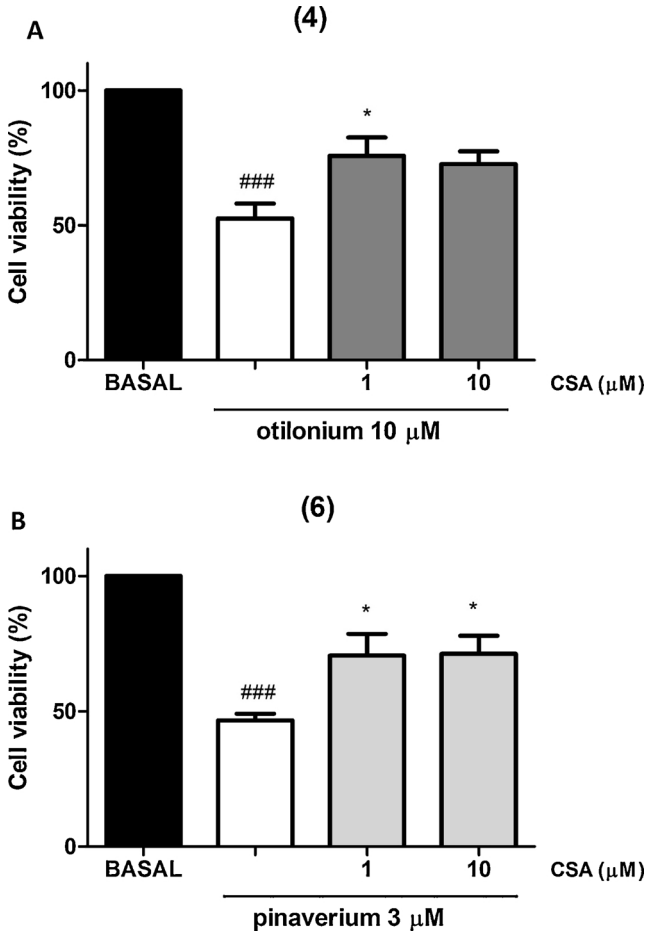

Fig. 6. Cyclosporine A (CSA) mitigates the neurotoxic effects of otilonium and pinaverium. After preincubation of CSA for 24 h at a concentration of 1 and 10 μM with the subsequent co-incubation for 24 h with otilonium at 10 μM (Panel A) or pinaverium at 3 μM (Panel B), viability was estimated with the MTT method. Data are means ± SEM of the number of experiments in triplicate shown in parentheses, done with different neuronal cultures. ###$p < 0.001$ with respect BASAL *$p < 0.05$ with respect the neurotoxic effects of OTI or PIN in the absence of CSA.

To this aim, neurons were preincubated with CSA (1 and 10 μM) for 24 h, followed by another 24 h period of co-incubation with CSA plus 10 μM otilonium or pinaverium. At the end of this second incubation period, cell viability was monitored with MTT.

In 4 triplicate experiments, otilonium elicited 47.4% of neuronal loss. In the presence of 1 μM CSA, however, neuronal loss was reduced by 51.2%. A similar neuroprotection was produced by 10 μM CSA, but it was at the limit of statistical significance (Fig. 6A). In the case of pinaverium, in 6 experiments the loss of neurons was 53.4%. This neuronal loss was reduced by 55.3% when pinaverium was co-incubated with 1 μM CSA; this neuroprotection was significant at the two CSA concentrations (Fig. 6B).

3.8. Effects of otilonium and pinaverium on neuronal death through necrosis and apoptosis pathways

So far we have monitored the viability of neurons with the MTT assay. This provides a useful information on mitochondrial activity and cell viability, but does not distinguish the possible mechanisms involved in cell death. Therefore, we planned this series of experiments to monitor the relative percentages of intact neurons and neurons that died by necrotic or apoptotic mechanisms; to this aim we used flow cytometry and specific death markers.

Most of the 20,000 labeled neurons explored with flow cytometry after their incubation for 24 h with Neurobasal medium were viable cells located in quadrant S3 (98.4% cells; annexin V-/7-AAD-) (Fig. 7A). A positive control using the pro-apoptotic agent staurosporin (Wu et al., 2014) was also done (Fig. 7B); in this case, most cells were located in quadrants S2 (68% early apoptosis and subsequent necrotic cell death; annexin V + /7-AAD -).

In Fig. 7 C,E the relative distribution of alive, necrotic and apoptotic neurons after their incubation during 24 h with increasing concentrations of otilonium or pinaverium (1–10 μM) are graphed. Note that the fraction of alive cells decreased as a function of drug concentration; however the percentage of apoptotic cells was increasing while the number of necrotic cells did not significantly change. For the sake of clarity, the fraction of apoptotic cells has been separately graphed in Fig. 7D (for otilonium) and 7 F (for pinaverium). Otilonium augmented the fraction of apoptotic cells at all concentrations but reached statistical significance with respect basal only at 10 μM. Also, pinaverium augmented apoptosis with significant outcomes at 3 and 10 μM.

3.9. Effects of Ac-LEHD-CHO and cyclosporine A on apoptotic neuronal death elicited by otilonium and pinaverium

Caspases, currently known as the central executors of the apoptotic pathway, are cysteine proteases that cleave substrates after aspartate residues and at least 14 different subtypes have been identified in mammalian cells (Cohen, 1997). Two pathways of caspase activation for apoptosis induction have been identified. The first one starts at death receptors such as Fas. In the second and more common pathway, diverse pro-apoptotic signals converge at the mitochondrial level, inducing the translocation of cytochrome c from mitochondria to cytosol, thus triggering the cascade of caspase activation. Caspase-3 is one of the most important active executors in the apoptosis pathway (Green and Reed, 1998). After neuronal pre-incubation with the inhibitor Ac-LEHD-CHO for 24 h, we co-incubated the cells with otilonium at 10 μM or pinaverium at 3 μM for an additional 24 h period after which flow cytometry was done. We found that the inhibitor of caspase-9 and caspase-3 managed to reverse cell death by otilonium (45% at 10 μM and 48% at 30 μM, Fig. 8A) and pinaverium (40% at 10 μM and 52% at 30 μM, Fig. 8B).

A similar experiment was performed with the mitochondrial mPTP blocker cyclosporine A (CSA). Once more, the protocol consisted in cell pre-incubation with CSA at 1 or 10 μM for 24 h followed by an additional 24 h period of co-incubation with CSA plus 10 μM otilonium or 3 μM pinaverium. Fig. 7C shows that CSA reduced by 53% at 1 μM and 60% at 10 μM the apoptotic neuronal death elicited by otilonium. The effect of CSA was much more drastic in the case of pinaverium as, at 1 μM, it caused 90% reduction of apoptosis and at 10 μM the reduction amounted to 77% (Fig. 8D).

To illustrate the neuroprotection exerted by CSA, we present in Fig. 9 a family of microphotographs of living neurons, incubated for increasing time period (0–24 h) with 10 μM otilonium or 3 μM pinaverium in the absence or the presence of CSA at 1 μM (protocol as in Fig. 8), with 24 h pre-incubation with CSA followed by incubation with otilonium or pinaverium for the different time periods. Note the healthy appearance of neurons incubated in basal conditions that exhibit abundant processes and that the plasma membrane is intact. After 2 h incubation with otilonium, neurons still showed a healthy appearance; however, those incubated with pinaverium already exhibited some damage with fewer processes. After 4–24 h incubation, the neuronal network appeared disorganized and most cells were round-shaped or were dead. In sharp contrast, the neuronal cultures incubated with CSA prior to the toxicant have most of their processes and the soma intact (two microphotograph columns at the right of Fig. 9).

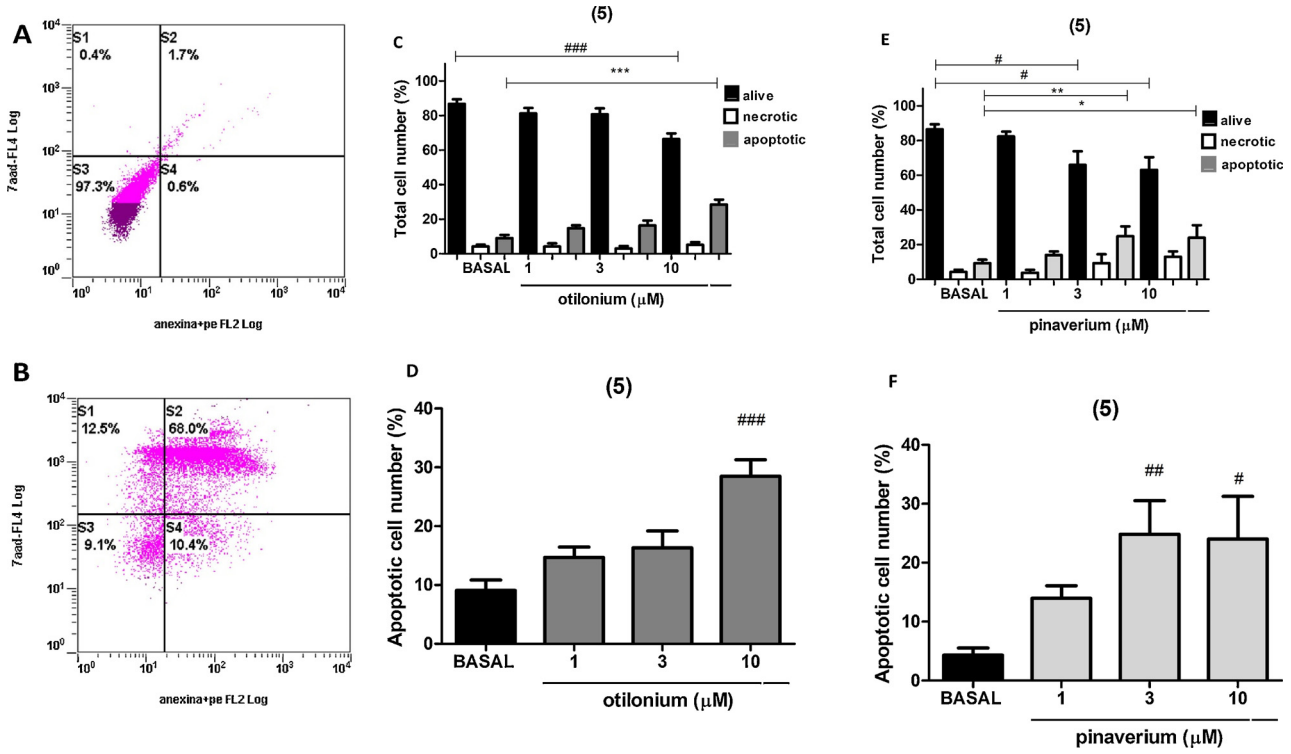

Fig. 7. Apoptotic versus necrotic cell death in neuronal cultures incubated with otilonium (OTI) or pinaverium during 24 h, at the concentrations shown in the abscissae of panels C,D,E,F. Relative percentages of alive, necrotic, and apoptotic cells at the end of the incubation period were determined with flow cytometry and selective double markers (see methods). A, Example flow cytometry recording of neurons under basal conditions; most cells were unlabeled and located in quadrant S3, indicating they are alive. B, Example of a positive control done with pro-apoptotic agent staurosporine; the majority of cells are marked with annexin V and they are located mostly in quadrant S2 (apoptotic cells). Panels C and E show the relative fraction of cells that after the 24 h incubation period with OTI or PIN, were alive, necrotic, or apoptotic. For the sake of clarity, apoptotic cells (% ordinates) are graphed in panels D (OTI) and F (PIN). Data are means ± SEM of 5 experiments in triplicate, statistical differences are calculated with respect basal. #p < 0.05, ##p < 0.01, ###p < 0.001 with respect BASAL and *p < 0.05 **p < 0.01, ***p < 0.001 respect with the neurotoxic drugs otilonium and pinaverium.

3.10. Effects of otilonium and pinaverium on the viability of bovine chromaffin cells and SH-SY5Y human neuroblastoma cells

These experiments were done to investigate whether the cytotoxic effects of otilonium and pinaverium were selective for the rat embryo cortical neurons or rather, they were also present in other cell types. To test this question, we selected sympathetic neuron-like adrenal medullary bovine chromaffin cells (BCCs) and the human neuroblastoma cell line SH-SY5Y. Experiments similar to those of Fig. 1 were done. After 24 h of cell incubation with 1–10 μM with otilonium and pinaverium, the MTT assay showed they elicited around 39–55% damage of BCCs at 10 μM; lower concentrations did not reduce cell viability (Fig. 10A,B). However, SH-SY5Y cells were resistant to damage after their incubation with otilonium or pinaverium for 24 h (Fig. 10C,D).

4. Discussion

Central to this investigation is the observation that otilonium and pinaverium elicited neurotoxic effects in primary cultures of rat embryo cortical neurons. Both drugs are known to relax the smooth muscle through a mechanism partly due to their ability to block muscarinic receptors (Maggi and Meli, 1983a; Malysz et al., 1997). Due to this pharmacological property, they were included in our repositioning programme with about 30 other cholinergic medicines that are also currently being used in different clinical contexts. Thus, we raised the possibility that their neurotoxic effects could be linked to their anti-muscarinic actions and then we tested other seven blockers of muscarinic receptors including classical atropine; they did not share with otilonium and pinaverium their neurotoxic effects (Fig. 2 A,B) and hence we are confident that those effect are unrelated to muscarinic receptor blockade. Nevertheless, as otilonium and pinaverium have a quaternary ammonium in their molecule, the suspicion arose that positively charged compounds could insert into the plasma membrane and/or react with surface lipids to elicit neurotoxicity (Joondan et al., 2015). This possibility may also be discarded on the basis of experiments with ten cholinergic drugs also having a quaternary ammonium in their molecular structure where, however, none of them exerted any significant neurotoxic actions (Fig. 2 C,D).

In this molecular structural context it is interesting to note that out of the 19 cholinergic drugs here tested, only otilonium and pinaverium have a long aliphatic chain (Fig. 2A). This may surely provide higher lipophilicity and greater capacity to insert into the plasma membrane. This is the case for some lipophilic blockers of VACCs such as flunarizine that can reach millimolar concentrations in cell membranes from concentrations in the low micromolar range in extracellular solutions (Scheufler and Peters, 1990). A priori one can guess that a link exists between the lipophilicity of a chemical and its potential to cause cell damage. In a previous report we tested 30 compounds and drugs in clinical use, to compare their log P (range -1.2 to 7.6) with their neurotoxic potential; but we found no correlation (Novalbos et al., 1999). The predicted value of log P for otilonium is 2.58 and the predicted log P for pinaverium is 0.53; thus, there is not an obvious correlation between lipophilicity and their ability to cause cell damage.

Blockade by otilonium of VACC currents (Fig. 3) and of K^+- elicited $[Ca^{2+}]_c$ transients (Fig. 4, and 5) corroborates its ability to block the whole-cell current through VACCs in bovine adrenal chromaffin cells as well as the K^+- evoked Ca^{2+} uptake into these cells (Gandia et al., 1996a,b). As bovine chromaffin cells express the neuronal L, N, and PQ subtypes of VACCs (Garcia et al., 2006), we may conclude that otilonium blocks those VACCS both in chromaffin cells and in neurons

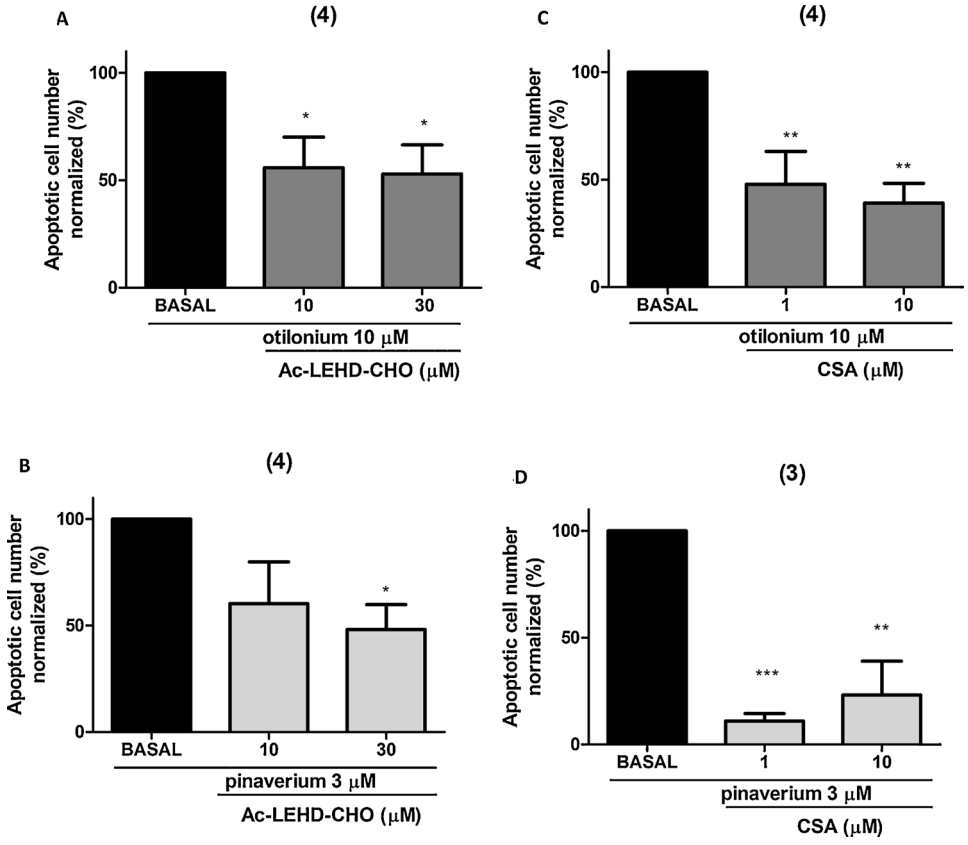

Fig. 8. The inhibitor Ac- LEHD-CHO of caspase 9 and caspase 3 as well as cyclosporine A (CSA) manage to reverse cell death by otilonium and pinaverium. After preincubation with Ac-LEHD-CHO at 10 and 30 μM or CSA at 1 or 10 μM for 24 h, a drastic reversal for apoptosis is shown, in the case of otilonium (Panel A, C) and pinaverium (Panel B, D). Data are means ± SEM of 3 or 4 triplicate experiments done with different cultures. *p < 0.05 **p < 0.01, ***p < 0.001, with respect BASAL .

(present study). As far as pinaverium in concerned, we are only aware of its ability to block the L-type VACCs of smooth muscle (Malysz et al., 1997). However, the fact that in this study pinaverium fully blocked the VACC currents and the K^+- elicited $[Ca^{2+}]_c$ transients (Figs. 3 to 5) suggests that as happens to be the case for otilonium, pinaverium also blocks L- as well as N- and PQ- subtypes of VACCs in neurons. Hence, it seems that we can include otilonium and pinaverium among a group of so-called "wide-spectrum" calcium channel blockers as flunarizine, cinnarizine, or dotarizine (Gandia et al., 1996b). In this frame, the question arises as to whether the capacity of otilonium and pinaverium to block the entry of Ca^{2+} through VACCs during cell depolarization and the ensuing reduction of the amplitude of $[Ca^{2+}]_c$ transient, are linked in some manner to their neurotoxic effects.

It is worth considering that cell death elicited by several toxic agents is dependent on cell Ca^{2+} overload (Choi, 1985; Schanne et al., 1979; Trump and Berezesky, 1995). Of note is also the fact that Ca^{2+} ions are involved in the production of reactive oxygen or nitrogen species (ROS, RNS), mitochondrial Ca^{2+} circulation and mitochondrial bioenergetics, acting as a mediator of cell energy demand and at the cell life/death cycle (Bhosale et al., 2015; Carraro and Bernardi, 2016; Garcia et al., 2012; Gorlach et al., 2015). Thus, we may arrive to the conclusion that the blockade of Ca^{2+} entry and the reduction of $[Ca^{2+}]_c$ levels during hours may underlie the neuronal damaging effects of otilonium and pinaverium. This hypothesis may explain why the experiments with free radical sequestering agents, namely NAC, melatonin, or catalase did not protect against the neurotoxic effects of otilonium or pinaverium (data not shown).

The interpretation we offer on the possibility that low $[Ca^{2+}]_c$ chronically maintained during hours in neurons incubated with otilonium or pinaverium, may enter in conflict with the generally accepted view that acute Ca^{2+} overload triggers mitochondrial ROS and the opening of mPTP, to activate the apoptotic cascade and cell death. In this manner by reducing $[Ca^{2+}]_c$ load, otilonium and pinaverium should had exerted a neuroprotective rather than a neurotoxic effect. Nevertheless, we may here bring about a second concept, opposite to that of cell Ca^{2+} load, the so-called "calcium set-point hypothesis": a minimal $[Ca^{2+}]_c$ level is required to maintain neuronal viability (Johnson et al., 1992; Orozco et al., 2006; Thompson et al., 2001). When the $[Ca^{2+}]_c$ moves below or above such set point, apoptosis is rapidly induced (Franklin and Johnson, 1994). This reminds some wide-spectrum calcium antagonists like flunarizine that drastically reduces the $[Ca^{2+}]_c$ levels and as otilonium and pinaverium, also causes cell death (Novalbos et al., 1999).

During cell activation, the large $[Ca^{2+}]_c$ loads are rapidly and efficiently cleared by mitochondria (Montero et al., 2000). This serves to modulate and shape these $[Ca^{2+}]_c$ transients as well as to couple the mitochondrial bioenergetics to cell activity (Duchen, 1999; Garcia et al., 2012). In the context of the set point hypothesis, it seems plausible that by maintaining the $[Ca^{2+}]_c$ levels below such set-point, the mitochondrial bioenergetics will be impaired; this could lead to mPTP pore opening, an action that is strongly supported by the clear neuroprotective effects afforded by cyclosporine A (Figs. 6 and 9), a blocker of mPTP (Fakharnia et al., 2017) against the neurotoxic effects of otilonium and pinaverium.

In the pro-apoptotic effects on otilonium and pinaverium it seems that the opening of the mPTP pore is involved; following this opening, cytochrome c is released into the cytosol through the opening of mPTP to form the apoptosome and the activation of cascade-9 and caspase-3 (Fernandez-Morales et al., 2012; Green and Reed, 1998). The fact Ac-LEHD-CHO, an inhibitor of caspase-9 and caspase-3 (Meller et al., 2006) protected against the neurotoxic effects of otilonium and pinaverium, supports the interpretation of our results in the sense that these two drugs, although acting indirectly by interfering with neuronal Ca^{2+} handling, are activating the intrinsic mitochondrially mediated apoptotic pathway in rat embryo cortical neurons.

Another interesting question is whether the neuronal cytotoxic effects of otilonium and pinaverium are a general cytotoxic action that affects other cell types. We were surprised to learn that bovine

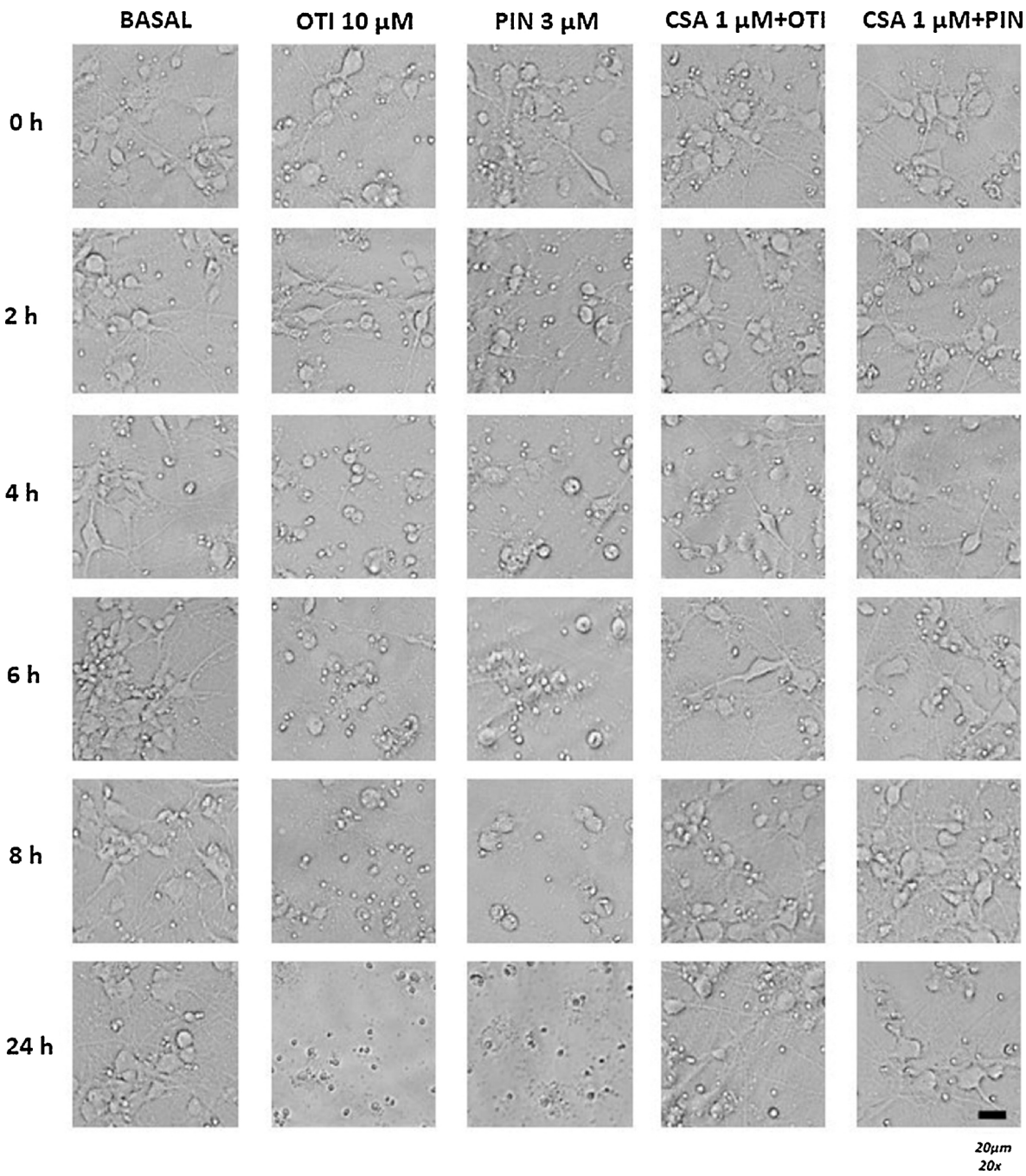

Fig. 9. Morphology of the reversal apoptosis process. This picture is composed of photographs at 20x magnification, made after cell preincubation with cyclosporine A (CSA) for 24 h and the co-incubation of otilonium (OTI 10 µM) or pinaverium (PIN 3 µM) for 24 additional h. It can be clearly observed that in the presence of OTI and PIN cells are damaged (from 4 h to 24 h incubation). The presence of CSA could prevent cell damage.

chromaffin cells and human neuroblastoma SH-SY5Y cells were substantially more resistant to the cytotoxic effects of the two drugs, in comparison with the more vulnerable cortical neurons. This may find an explanation in the fact that bovine chromaffin cells and undifferentiated SH-SY5Y cells may express different subtypes of VACCs, compared with cortical neurons (Garcia et al., 2006).

Finally, we would like to raise some clinical considerations emanating from our present work. In an early study we found that otilonium was a potent blocker of the neuronal-type nicotinic receptors for ACh (nAChRs) in bovine chromaffin cells. In that study we suggested that by also blocking the nAChRs of parasympathetic ganglia at the Auerbach plexus, in addition to its antimuscarinic effects and the blockade of VACCs, otilonium could exert its enteric spasmolytic effects with more efficiency (Gandia et al., 1996b). This could also be the case for pinaverium, although data on whether it blocks nAChRs are not available. In any case, the quaternary ammonium in their molecule precludes their systemic absorption from the gastro-intestinal lumen, to elicit neuronal toxicity as proven by the fact they have been safely and orally used to treat various gastrointestinal disorders including irritable bowel syndrome (Barbara et al., 1991; Ford et al., 2018; Giachetti, 1991; Lovell and Ford, 2012).

5. Conclusions

In conclusion, we here show that antimuscarinic spasmolytic drugs otilonium and pinaverium cause cell death in primary cultures of rat

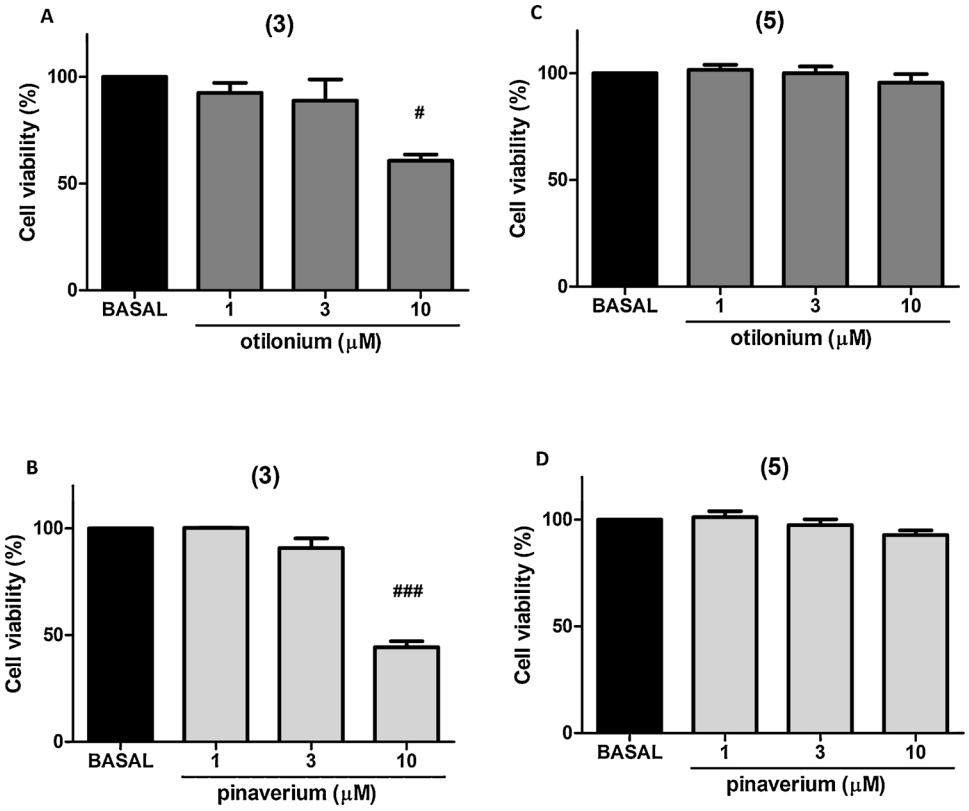

Fig. 10. Lesser or no damage exerted by otilonium and pinaverium on bovine chromaffin cells (A,B) and human neuroblastoma SH-SY5Ycells (C,D). Protocols consisted in cell incubation during 24-h with increasing concentrations of the drugs (abscissae) and after this period, cell viability was monitored with MTT (ordinates). Data are means ± SEM of the number of triplicate experiments with cells from different cultures shown in parentheses. #p < 0.05, ###p < 0.001 with respect normalized BASAL viability.

embryo cortical neurons through the indirect activation, by disturbed cell Ca^{2+} handling, of the intrinsic mitochondrially linked apoptotic pathway. We attribute this to their ability to block calcium channels thus preventing calcium entry. In doing so, otilonium and pinaverium will uncouple the calcium-dependent mitochondrial bioenergetics, causing this way the opening of mitochondrial mPTP, the activation of caspase-9 and caspase-3, and the triggering of apoptosis. Since these drugs are orally administered and they have a quaternary ammonium in their molecule, it is highly unlikely that our in vitro results impact on the long standing clinical safety of pinaverium and otilonium in the treatment of patients suffering of irritable bowel syndrome (Ford et al., 2018). Our results also suggest that otilonium and pinaverium (and particularly the last one) could serve as experimental tools to explore the mechanisms underlying neuronal apoptosis linked to the chronic blockade of Ca^{2+} entry through VACCs.

Acknowledgments

Supported by the following grants: MINECO 2016-78892-R. (2) European Union Horizon 2020 Research and Innovation Programme under the Marie Skoldowska-Curie Grant Agreement No 766124; (3) Cátedra CABICYC UAM-Bioibérica; (4) Cátedra Nutrinfant UAM-Alter. We also thank the continued support of Fundación Teófilo Hernando.

References

Barbara, L., Baldi, F., Longanesi, A., 1991. Pathogenesis of irritable bowel syndrome. Ital. J. Gastroenterol. 23 (8 Suppl 1), 36–38.
Bhosale, G., Sharpe, J.A., Sundier, S.Y., Duchen, M.R., 2015. Calcium signaling as a mediator of cell energy demand and a trigger to cell death. Ann. N. Y. Acad. Sci. 1350, 107–116.
Bobo, M.H., Magous, R., Christen, M.O., Bali, J.P., 1994. Effect of pinaverium and other calcium channel blockers on contraction of isolated gastric antral smooth muscle cells caused by gastrointestinal hormones. Life Sci. 54 (25), 1947–1954.
Bouchoucha, M., Faye, A., Devroede, G., Arsac, M., 2000. Effects of oral pinaverium bromide on colonic response to food in irritable bowel syndrome patients. Biomed. Pharmacother. 54 (7), 381–387.
Carraro, M., Bernardi, P., 2016. Calcium and reactive oxygen species in regulation of the mitochondrial permeability transition and of programmed cell death in yeast. Cell Calcium 60 (2), 102–107.
Cipriani, G., Gibbons, S.J., Saravanaperumal, S.A., Malysz, J., Sha, L., Szurszewski, J.H., Linden, D.R., Evangelista, S., Faussone-Pellegrini, M.S., Vannucchi, M.G., Farrugia, G., 2015. Changes in nitrergic and tachykininergic pathways in rat proximal colon in response to chronic treatment with otilonium bromide. Neurogastroenterol. Motil. 27 (7), 997–1009.
Cohen, G.M., 1997. Caspases: the executioners of apoptosis. Biochem. J. 326 (Pt 1), 1–16.
Choi, D.W., 1985. Glutamate neurotoxicity in cortical cell culture is calcium dependent. Neurosci. Lett. 58 (3), 293–297.
Duchen, M.R., 1999. Contributions of mitochondria to animal physiology: from homeostatic sensor to calcium signalling and cell death. J. Physiol. 516 (Pt 1), 1–17.
Evangelista, S., Traini, C., Vannucchi, M.G., 2018. Otilonium bromide: a drug with a complex mechanism of action. Curr. Pharm. Des.
Fakharnia, F., Khodagholi, F., Dargahi, L., Ahmadiani, A., 2017. Prevention of cyclophilin D-mediated mPTP opening using cyclosporine-A alleviates the elevation of necroptosis, autophagy and apoptosis-related markers following Global Cerebral Ischemia-Reperfusion. J. Mol. Neurosci. 61 (1), 52–60.
Fernandez-Morales, J.C., Arranz-Tagarro, J.A., Calvo-Gallardo, E., Maroto, M., Padin, J.F., Garcia, A.G., 2012. Stabilizers of neuronal and mitochondrial calcium cycling as a strategy for developing a medicine for Alzheimer's disease. ACS Chem. Neurosci. 3 (11), 873–883.
Feron, O., Wibo, M., Christen, M.O., Godfraind, T., 1992. Interaction of pinaverium (a quaternary ammonium compound) with 1,4-dihydropyridine binding sites in rat ileum smooth muscle. Br. J. Pharmacol. 105 (2), 480–484.
Ford, A.C., Lacy, B.E., Harris, L.A., Quigley, E.M., Moayyedi, P., 2018. Effect of antidepressants and psychological therapies in irritable bowel syndrome: an updated systematic review and meta-analysis. Am. J. Gastroenterol (in press).
Franklin, J.L., Johnson Jr, E.M., 1994. Elevated intracellular calcium blocks programmed neuronal death. Ann. N. Y. Acad. Sci. 747, 195–204.
Gandia, L., Lopez, M.G., Villarroya, M., Gilabert, J.A., Cardenas, A., Garcia, A.G., Borges, R., 1996a. Blocking effects of otilonium on Ca^{2+} channels and secretion in rat chromaffin cells. Eur. J. Pharmacol. 298 (2), 199–205.
Gandia, L., Villarroya, M., Lara, B., Olmos, V., Gilabert, J.A., Lopez, M.G., Martinez-Sierra, R., Borges, R., Garcia, A.G., 1996b. Otilonium: a potent blocker of neuronal nicotinic ACh receptors in bovine chromaffin cells. Br. J. Pharmacol. 117 (3), 463–470.
Garcia, A.G., Garcia-De-Diego, A.M., Gandia, L., Borges, R., Garcia-Sancho, J., 2006. Calcium signaling and exocytosis in adrenal chromaffin cells. Physiol. Rev. 86 (4), 1093–1131.
Garcia, A.G., Padin, F., Fernandez-Morales, J.C., Maroto, M., Garcia-Sancho, J., 2012. Cytosolic organelles shape calcium signals and exo-endocytotic responses of chromaffin cells. Cell Calcium 51 (3-4), 309–320.
Giachetti, A., 1991. Pharmacological studies on otilonium bromide. Ital. J. Gastroenterol. 23 (8 Suppl 1), 56–59.
Gorlach, A., Bertram, K., Hudecova, S., Krizanova, O., 2015. Calcium and ROS: a mutual

interplay. Redox Biol. 6, 260–271.
Green, D.R., Reed, J.C., 1998. Mitochondria and apoptosis. Science 281 (5381), 1309–1312.
Hamill, O.P., Marty, A., Neher, E., Sakmann, B., Sigworth, F.J., 1981. Improved patch-clamp techniques for high-resolution current recording from cells and cell-free membrane patches. Pflugers Arch. 391 (2), 85–100.
Johnson Jr, E.M., Koike, T., Franklin, J., 1992. A "calcium set-point hypothesis" of neuronal dependence on neurotrophic factor. Exp. Neurol. 115 (1), 163–166.
Joondan, N., Caumul, P., Akerman, M., Jhaumeer-Laulloo, S., 2015. Synthesis, micellisation and interaction of novel quaternary ammonium compounds derived from l-Phenylalanine with 1,2-dipalmitoyl-sn-glycero-3-phosphocholine as model membrane in relation to their antibacterial activity, and their selectivity over human red blood cells. Bioorg. Chem. 58, 117–129.
Lovell, R.M., Ford, A.C., 2012. Global prevalence of and risk factors for irritable bowel syndrome: a meta-analysis. Clin. Gastroenterol. Hepatol. 10 (7), 712–721 e714.
Maggi, C.A., Meli, A., 1983a. Assessment of potential selectivity of antispasmodics for the various sections of the gastrointestinal tract of the rat as a guideline for their clinical use. Arch. Int. Pharmacodyn. Ther. 262 (2), 221–231.
Maggi, C.A., Meli, A., 1983b. Reserpine-induced detrusor hyperreflexia: an in vivo model for studying smooth muscle relaxants at urinary bladder level. J. Pharmacol. Methods 10 (2), 79–91.
Malysz, J., Farraway, L.A., Christen, M.O., Huizinga, J.D., 1997. Pinaverium acts as L-type calcium channel blocker on smooth muscle of colon. Can. J. Physiol. Pharmacol. 75 (8), 969–975.
Martinez-Cutillas, M., Gil, V., Gallego, D., Mane, N., Martin, M.T., Jimenez, M., 2013. Mechanisms of action of otilonium bromide (OB) in human cultured smooth muscle cells and rat colonic strips. Neurogastroenterol. Motil. 25 (12), e803–812.
Meller, R., Clayton, C., Torrey, D.J., Schindler, C.K., Lan, J.Q., Cameron, J.A., Chu, X.P., Xiong, Z.G., Simon, R.P., Henshall, D.C., 2006. Activation of the caspase 8 pathway mediates seizure-induced cell death in cultured hippocampal neurons. Epilepsy Res. 70 (1), 3–14.
Montero, M., Alonso, M.T., Carnicero, E., Cuchillo-Ibanez, I., Albillos, A., Garcia, A.G., Garcia-Sancho, J., Alvarez, J., 2000. Chromaffin-cell stimulation triggers fast millimolar mitochondrial Ca^{2+} transients that modulate secretion. Nat. Cell Biol. 2 (2), 57–61.
Moro, M.A., Lopez, M.G., Gandia, L., Michelena, P., Garcia, A.G., 1990. Separation and culture of living adrenaline- and noradrenaline-containing cells from bovine adrenal medullae. Anal. Biochem. 185 (2), 243–248.
Mosmann, T., 1983. Rapid colorimetric assay for cellular growth and survival: application to proliferation and cytotoxicity assays. J. Immunol. Methods 65 (1-2), 55–63.
Novalbos, J., Abad-Santos, F., Zapater, P., Cano-Abad, M.F., Moradiellos, J., Sanchez-Garcia, P., Garcia, A.G., 1999. Effects of dotarizine and flunarizine on chromaffin cell viability and cytosolic Ca^{2+}. Eur. J. Pharmacol. 366 (2-3), 309–317.
Orozco, C., Garcia-de-Diego, A.M., Arias, E., Hernandez-Guijo, J.M., Garcia, A.G., Villarroya, M., Lopez, M.G., 2006. Depolarization preconditioning produces cytoprotection against veratridine-induced chromaffin cell death. Eur. J. Pharmacol. 553 (1-3), 28–38.
Osman, M.M., Lulic, D., Glover, L., Stahl, C.E., Lau, T., van Loveren, H., Borlongan, C.V., 2011. Cyclosporine-A as a neuroprotective agent against stroke: its translation from laboratory research to clinical application. Neuropeptides 45 (6), 359–368.
Santicioli, P., Zagorodnyuk, V., Renzetti, A.R., Maggi, C.A., 1999. Antimuscarinic, calcium channel blocker and tachykinin NK2 receptor antagonist actions of otilonium bromide in the circular muscle of guinea-pig colon. Naunyn Schmiedebergs Arch. Pharmacol. 359 (5), 420–427.
Schanne, F.A., Kane, A.B., Young, E.E., Farber, J.L., 1979. Calcium dependence of toxic cell death: a final common pathway. Science 206 (4419), 700–702.
Scheufler, E., Peters, T., 1990. Phosphatidylserine monolayers as models for drug uptake into membranes and tissue. Cell Biol. Int. Rep. 14 (4), 381–388.
Schmid, I., Krall, W.J., Uittenbogaart, C.H., Braun, J., Giorgi, J.V., 1992. Dead cell discrimination with 7-amino-actinomycin D in combination with dual color immunofluorescence in single laser flow cytometry. Cytometry 13 (2), 204–208.
Thompson, G.J., Langlais, C., Cain, K., Conley, E.C., Cohen, G.M., 2001. Elevated extracellular $[K^+]$ inhibits death-receptor- and chemical-mediated apoptosis prior to caspase activation and cytochrome c release. Biochem. J. 357 (Pt 1), 137–145.
Traini, C., Evangelista, S., Girod, V., Faussone-Pellegrini, M.S., Vannucchi, M.G., 2017. Repeated otilonium bromide administration prevents neurotransmitter changes in colon of rats underwent to wrap restraint stress. J. Cell. Mol. Med. 21 (4), 735–745.
Trump, B.F., Berezesky, I.K., 1995. Calcium-mediated cell injury and cell death. FASEB J. 9 (2), 219–228.
Wu, J., Wang, Y., Liang, S., Ma, H., 2014. Cytoprotective effect of selective small-molecule caspase inhibitors against staurosporine-induced apoptosis. Drug Des. Devel. Ther. 8, 583–600.